

## Molecular Wiring of LiFePO<sub>4</sub> (Olivine)

Ladislav Kavan,<sup>\*,†</sup> Ivan Exnar,<sup>‡</sup> and Michael Graetzel<sup>§</sup>

*J. Heyrovský Institute of Physical Chemistry, v.v.i., Academy of Sciences of the Czech Republic, Dolejškova 3, CZ-18223 Prague 8, Czech Republic, High Power Lithium, SA, PSE-B, Ecublens, CH-1015 Lausanne, Switzerland, and Laboratory of Photonics and Interfaces, EPFL, Ecublens, CH-1015 Lausanne, Switzerland*

Received January 8, 2008

The carbon-free LiFePO<sub>4</sub> (olivine) was modified by a monolayer coverage with [12-(2,5-di-*tert*-butyl-4-methoxy-phenoxy)-dodecyl]-phosphonic acid, coded DW. Thin film electrodes were bonded with 5% PVDF and deposited on F-doped SnO<sub>2</sub> (FTO) support. The surface-modified LiFePO<sub>4</sub> can be electrochemically charged via a mechanism called molecular wiring. The DW molecules contacting FTO are reversibly oxidized, which allows that the holes are transported from the FTO via the adsorbed DW monolayer across the whole olivine surface, where a subsequent chemical delithiation occurs toward FePO<sub>4</sub>. The sole cross-surface hole percolation via adsorbed DW was demonstrated on two reference systems, namely, TiO<sub>2</sub> and LiMnPO<sub>4</sub> (olivine), which are electrochemically inert in the potential region, where the DW oxidation occurs. The diffusion coefficient of hole transport across the LiMnPO<sub>4</sub> surface equals  $3 \times 10^{-9}$  cm<sup>2</sup>/s, which is ca. three times larger than the corresponding value for mesoporous TiO<sub>2</sub>. The undoped and carbon-free LiFePO<sub>4</sub> can be charged by currents equivalent to ca. C/2 to C/10 exclusively via the monolayer of adsorbed molecules, but the process slows down when the charging progresses. The wiring current is roughly inversely proportional to the level of olivine charging by oxidative delithiation.

### Introduction

Since the pioneering work of Goodenough et al.,<sup>1</sup> LiFePO<sub>4</sub> (olivine) attracted considerable interest for application as a cathode material in Li-ion batteries with improved safety and reduced cost. However, the poor electrical conductivity of LiFePO<sub>4</sub> is a crucial issue to be addressed<sup>2</sup> either by doping with supervalent cations<sup>3</sup> or by carbon additives, which may also generate iron phosphides or phosphocarbides at the surface.<sup>4</sup> Various strategies of conductivity promoting have also raised conflicting debate in the literature,<sup>5</sup> and eventually, the strain generated during the charge/discharge needs to be considered as another factor controlling the performance of olivine structures.<sup>5</sup> The classical core–shell model with interfacial solid solution of Li<sub>x</sub>FePO<sub>4</sub> has been recently replaced by a model of two-phase conversion of LiFePO<sub>4</sub>/FePO<sub>4</sub> with Li<sup>+</sup> ions moving parallel to the *b*-axis of the olivine lattice.<sup>6,7</sup>

Graetzel et al.<sup>8,9</sup> have developed two novel strategies for charging/discharging of stoichiometric LiFePO<sub>4</sub> (doping- and carbon-free), which are called molecular wiring<sup>8</sup> and redox targeting.<sup>9</sup> They are both based on hole/electron transport from a current collector via a redox active molecule interacting with the LiFePO<sub>4</sub> cathode. In the first case, the redox relay molecule is chemically anchored to the LiFePO<sub>4</sub> surface;<sup>8</sup> in the second case the relay molecule is freely diffusing in the electrolyte solution.<sup>9</sup> The redox targeting obviously asks for a special separator preventing that the redox molecule contacts the counter-electrode. In the absence of this separator, the relay molecule gets reduced on the counter-electrode instead of causing oxidative delithiation of LiFePO<sub>4</sub>. Such a self-discharge is undesired for redox targeting, but it can be actually beneficial for another application, namely, overcharge protection via a redox shuttle.<sup>10</sup> In this case, the redox shuttle molecule accommodates the overcharge current on the LiFePO<sub>4</sub> cathode and bypasses it to the anode via the electrolyte solution.

Systematic investigation of this phenomenon by Dahn et al.<sup>11–13</sup> pointed out that there are only few redox-shuttle molecules that are stable enough to prevent overcharging of

\* Corresponding author. E-mail: kavan@jh-inst.cas.cz.

† Academy of Sciences of the Czech Republic.

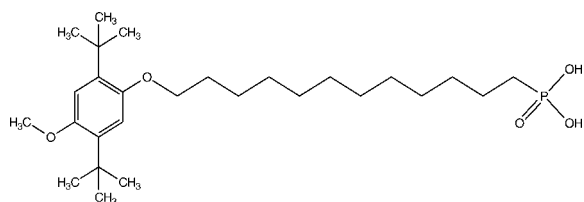
‡ PSE-B.

§ EPFL.

- (1) Padhi, A. K.; Nanjundasawamy, K. S.; Goodenough, J. B. *J. Electrochem. Soc.* **1997**, *144*, 1188.
- (2) Ellis, B.; Perry, L. K.; Ryan, D. H.; Nazar, L. F. *J. Am. Chem. Soc.* **2006**, *128*.
- (3) Chung, S. Y.; Bloking, J. T.; Chiang, Y. M. *Nat. Mater.* **2002**, *1*, 123.
- (4) Herle, P. S.; Ellis, B.; Coombs, N.; Nazar, L. F. *Nat. Mater.* **2004**, *3*, 147.
- (5) Meetlong, N.; Huang, H.Y.J.S.; Speakman, S. A.; Carter, W. C.; Chiang, Y. M. *Adv. Funct. Mater.* **2007**, *17*, 1115.
- (6) Chen, G.; Song, X.; Richardson, T. J. *Electrochem. Solid State Lett.* **2006**, *9*, A295.
- (7) Laffont, L.; Delacourt, C.; Gibot, P.; Wu, M. Y.; Koyman, P.; Masquelier, C.; Tarascon, J. M. *Chem. Mater.* **2006**, *18*, 5520.

- (8) Wang, Q.; Evans, N.; Zakeeruddin, S. M.; Exnar, I.; Grätzel, M. *J. Am. Chem. Soc.* **2007**, *128*, 3163.
- (9) Wang, Q.; Zakeeruddin, S. M.; Wang, D.; Exnar, I.; Grätzel, M. *Angew. Chem.* **2006**, *118*, 8377.
- (10) Chen, J.; Buhrmester, C.; Dahn, J. R. *Electrochem. Solid State Lett.* **2005**, *8*, A59.
- (11) Buhrmester, C.; Chen, J.; Moshurchak, L.; Jiang, J.; Wang, R. L.; Dahn, J. R. *J. Electrochem. Soc.* **2005**, *152*, A2390.
- (12) Moshurchak, L.; Buhrmester, C.; Wang, R. L.; Dahn, J. R. *Electrochim. Acta* **2007**, *52*, 3779.
- (13) Moshurchak, L.; Buhrmester, C.; Dahn, J. R. *J. Electrochem. Soc.* **2008**, *155*, A129.

Scheme 1. Formula of DW



the  $\text{LiFePO}_4$  cathode under its operating conditions in the Li-ion battery. Three types of molecules showed overcharge protection for more than 100 cycles: derivatives of 2,2,6,6-tetramethylpiperidyl oxide, phenothiazine, and 2,5-di-*tert*-butyl-1,4-dimethoxy benzene (DDB), the latter being the most stable redox shuttle ever reported.<sup>11,12</sup>

In this paper, we have utilized the exceptional stability of DDB for exploring its possible application in molecular wiring. Since DDB is not chemisorbed on the olivine surface, we had to modify its structure by a molecular linker, namely, a  $\text{C}_{12}$ -aliphatic chain terminated by a phosphonic acid group,  $-\text{PO}_3\text{H}_2$ . The latter serves for anchoring of the redox-active molecule to the  $\text{LiFePO}_4$  surface. For instance, 4-[bis(4-methoxyphenyl)amino]benzylphosphonic acid (BMABP) is strongly adsorbed to  $\text{LiFePO}_4$ ; the reaction follows a Langmuir adsorption isotherm with an adsorption equilibrium constant of  $1.35 \times 10^5 \text{ M}^{-1}$ .<sup>8</sup> Our molecule, [12-(2,5-di-*tert*-butyl-4-methoxy-phenoxy)-dodecyl]-phosphonic acid, is expected to have both the beneficial properties of DDB and BMABP, namely, good redox stability and strong anchoring to the olivine surface. This molecule is further coded DW (Scheme 1).

## Experimental Section

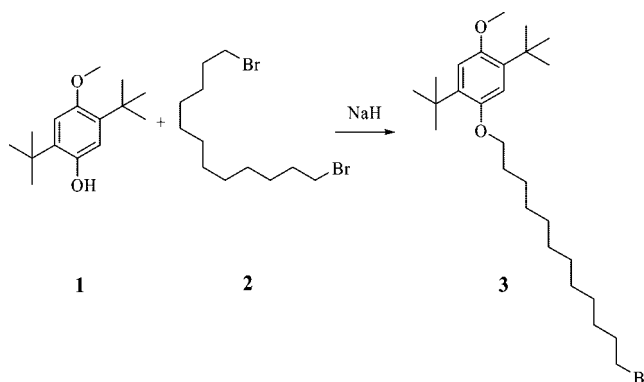
The carbon-free  $\text{LiFePO}_4$  (olivine) was obtained from Süd-Chemie, AG (lot no. EXM 1195-T22). The nitrogen adsorption isotherms indicated its BET surface area to be  $9 \text{ m}^2/\text{g}$ . Electrodes were prepared by mixing the powder of  $\text{LiFePO}_4$  with 5 wt % of poly(vinylidene fluoride) (PVDF) dissolved in *N*-methyl-2-pyrrolidone. The resulting homogeneous slurry was then doctor-bladed onto F-doped conducting glass (FTO;  $15 \Omega/\text{sq}$ ), and the film was cut into smaller pieces of  $0.8\text{--}1 \text{ cm}^2$  area and dried at  $100 \text{ }^\circ\text{C}$  overnight. Uncovered area at the edge of the FTO support served for electrical contacting. The typical film mass was  $2.4\text{--}3.2 \text{ mg}/\text{cm}^2$ .  $\text{LiMnPO}_4$  (BET surface area of  $35 \text{ m}^2/\text{g}$ ) was made via the "polyol" route by HPL.<sup>14</sup> The PVDF-bonded film from  $\text{LiMnPO}_4$  was prepared in the same way; the film mass was  $1.1\text{--}1.7 \text{ mg}/\text{cm}^2$ . Mesoscopic  $\text{TiO}_2$  film was prepared as in ref 15; it consisted of 20-nm anatase particles, and the  $\text{TiO}_2$  film thickness was  $2.5 \mu\text{m}$ , porosity 0.63, and roughness factor  $\approx 110$  per micrometer. The projected area of the  $\text{TiO}_2$  film was  $0.2 \text{ cm}^2$ .

DW was synthesized via two intermediates (**3** and **4**) as follows:

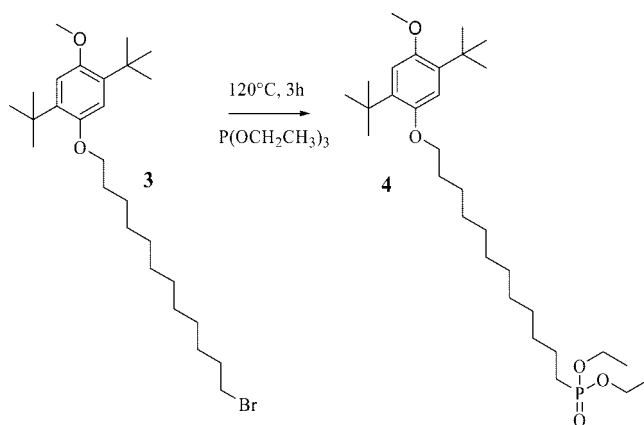
**Intermediate 3.** 1-(12-Bromododecyloxy)-2,5-di-*tert*-butyl-4-methoxybenzene was prepared by a modified procedure from ref 16 (Scheme 2).

A total of 0.11 g of NaH in 15 mL of anhydrous tetrahydrofuran (THF) was mixed with 1 g (4.23 mmol) of **1**. A gas evolution occurred for a few minutes, and when it was finished 3.5 g (10 mmol) of 1,12-dibromododecane (dissolved in 15 mL of THF) was added. The mixture was stirred at room temperature for about 1 h,

Scheme 2. Synthesis of the Intermediate 3



Scheme 3. Synthesis of the intermediate 4



and then the system was refluxed for 20 h in the dark under argon atmosphere. The mixture was cooled to room temperature, and 60 mL of water was added. The organic phase was extracted with dichloromethane ( $3 \times 60 \text{ mL}$ ) and dried with  $\text{CaCl}_2$ , and the solvent was removed under vacuum to give a slightly yellow viscous liquid. The product was purified by flash chromatography on silica gel (ethyl acetate/petroleum ether 5:95), giving 1.7 g of pure (GC/MS) product in the form of colorless liquid. Yield: 83%. MS (EI): 482 (M+), 484 (M+2), 236; 221 (100%).  $^1\text{H NMR}$  ( $\text{CDCl}_3$ , t.a.): 1.28–1.32 ppm (bm, 36H, H chain +  $\text{C}(\text{CH}_3)_3$ ); 1.81 ppm (bm, 4H, H chain); 3.76 ppm (s, 3H,  $\text{OCH}_3$ ); 3.90 ppm (t, 2H,  $\text{OCH}_2\text{CH}_2$ ); 4.10 ppm (t, 2H,  $\text{CH}_2\text{Br}$ ); 6.81 ppm (bs, 2H,  $\text{H}_{\text{ar}}$ ).

**Intermediate 4.** Diethyl-12-(2,5-di-*tert*-butyl-4-methoxyphenoxy)dodecylphosphonate was prepared from intermediate **3** as follows (Scheme 3).

One gram of intermediate **3** was dissolved in 8 mL of triethylphosphite and stirred at  $120 \text{ }^\circ\text{C}$  for about 3 h in the dark under argon. Then the excess of triethylphosphite was distilled off at reduced pressure, and the product collected as brown liquid. The purification was carried out by flash chromatography on silica gel (petroleum ether/ethyl acetate 5:1). The product is a colorless liquid (Yield: 85%). MS (EI): 540 (M+); 305 (100%).  $^1\text{H NMR}$  ( $\text{CDCl}_3$ ): 1.18–1.35 ppm (bm, 42H, H chain +  $\text{POCH}_2\text{CH}_3$  +  $\text{C}(\text{CH}_3)_3$ ); 1.71 ppm (m, 2H, H chain); 1.81 ppm (m, 4H, H chain); 3.80 ppm (s, 3H,  $\text{OCH}_3$ ); 3.94 ppm (t, 2H,  $\text{OCH}_2\text{CH}_2$ ); 4.09 ppm (m, 4H,  $\text{POCH}_2\text{CH}_3$ ); 6.81 ppm (d, 2H,  $\text{H}_{\text{ar}}$ ).

The target molecule, 12-(2,5-di-*tert*-butyl-4-methoxyphenoxy)-dodecylphosphonic acid (DW), was synthesized from 0.5 g of intermediate **4** dissolved in 15 mL of aqueous 12 N HCl. The solution was stirred at reflux temperature overnight in the dark. The reaction was followed by  $^1\text{H-NMR}$  until the signal of  $\text{CH}_2$  of the esters had disappeared. Then the excess of hydrochloric acid was distilled off at reduced pressure, and the product collected as

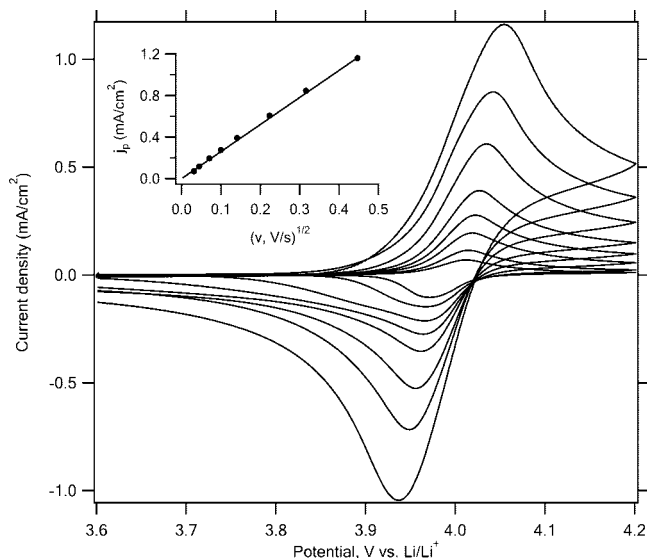


**Figure 1.** Cyclic voltammograms of DW adsorbed on a mesoporous TiO<sub>2</sub> film. Scan rates (in mV/s): 200, 100, 50, 20, 10, 5, 2, 1. Inset shows the forward peak current as a function of the square root of the scan rate.

brown viscous oil. The product was dissolved three times in toluene, and the solvent was distilled off at reduced pressure. No other purification was needed. Yield: quantitative. <sup>1</sup>H NMR (CDCl<sub>3</sub>): 1.18–1.35 ppm (bm, 36H, H chain + C(CH<sub>3</sub>)<sub>3</sub>); 1.48 ppm (m, 2H, H chain); 1.81 ppm (m, 4H, H chain); 3.80 ppm (s, 3H, OCH<sub>3</sub>); 3.94 ppm (t, 2H, OCH<sub>2</sub>CH<sub>2</sub>); 6.81 ppm (d, 2H, H<sub>ar</sub>).

Anchoring of DW onto the olivine surface was carried out by dipping the electrode overnight into 10<sup>-3</sup> mol/L solution of DW in hexane. The surface coverage of the electrode material with DW was determined spectrophotometrically. The concentration difference of the DW/hexane solution was measured before and after the adsorption using the UV absorption peak of DW at λ = 288 nm. The derivatized electrode was rinsed with hexane to remove any weakly adsorbed DW and dried in vacuum at room temperature.

Electrochemical experiments employed an Autolab PGSTAT potentiostat (Ecochemie) controlled by the GPES 4 software. The electrolyte solution was 1 mol/L LiPF<sub>6</sub> in ethylene carbonate + propylene carbonate + dimethylcarbonate (EC/PC/DMC; 1/1/3; w). The reference and counter electrodes were from Li metal; hence, all potentials are quoted against the Li/Li<sup>+</sup> reference electrode in this medium. All electrochemical measurements were carried out in a glovebox under Ar atmosphere.

## Results and Discussion

Figure 1 shows the cyclic voltammogram of DW adsorbed on the mesoscopic TiO<sub>2</sub> electrode. DW exhibits a reversible charge-transfer reaction, despite the TiO<sub>2</sub> is insulating in this potential region and inactive for any (dark) electrochemistry. This is evidence for cross-surface electron/hole percolation in the self-assembled monolayer of DW molecules.<sup>15</sup> UV spectrophotometry indicated the surface coverage of TiO<sub>2</sub> with DW to be 0.3 nmol/cm<sup>2</sup>, which equals ≈2 molecules/nm<sup>2</sup>. (The coverage is referenced to the overall physical (BET) surface area of the electrode material, which was 55 cm<sup>2</sup>; see Experimental Section for details.) The integrated voltammetric charge at the slowest scan (1 mV/s) was 1.51 mC, which translates into 0.28 nmol/cm<sup>2</sup>. Hence, the DW

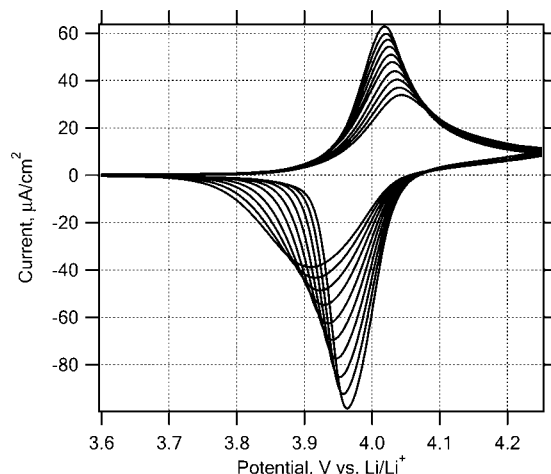


**Figure 2.** Cyclic voltammograms of DW adsorbed on a mesoporous TiO<sub>2</sub> film. Scan rate 1 mV/s. Ten successive scans were accumulated.

makes roughly a monolayer on the TiO<sub>2</sub> surface and is fully active for ambipolar charge transport from the FTO support. The inset in Figure 1 shows that the forward peak current density,  $J_p$  scales with the square root of the scan rate,  $v^{1/2}$ , according to the Randles–Sevcik equation:<sup>15</sup>

$$J_p = 0.4463nFc_0(nF/RT)^{1/2}D_+v^{1/2} \quad (1)$$

( $n$  is number of electrons, and the other symbols have their usual meaning). The concentration of DW in the film (thickness 2.5 μm) equals  $c_0 = 3.3 \times 10^{-4}$  mol/cm<sup>3</sup>. From the slope of the line in Figure 1 (inset) and eq 1 we can calculate the diffusion coefficient  $D_+ = 9 \times 10^{-10}$  cm<sup>2</sup>/s. This coefficient describes the cross surface motion of holes through the DW monolayer but not the mass transport, because the translational motion of chemisorbed molecules is excluded. More precisely,  $D_+$  is an ambipolar diffusion coefficient which reflects both the motion of holes at the surface and that of charge compensating counterions in the electrolyte solution. This charge transfer stops below the percolation threshold (ca. 50% coverage by the relay molecule).<sup>15</sup> The found  $D_+$  is not too far from the value for the Ru-bipyridine complex Z-907 adsorbed on TiO<sub>2</sub> [ $D_+ = (1.5\text{--}4.1) \times 10^{-9}$  cm<sup>2</sup>/s]<sup>15</sup> but is 3 orders of magnitude smaller than the value of “real” diffusion coefficient of DDB dissolved in electrolyte solution ( $1.6 \times 10^{-6}$  cm<sup>2</sup>/s).<sup>17</sup>

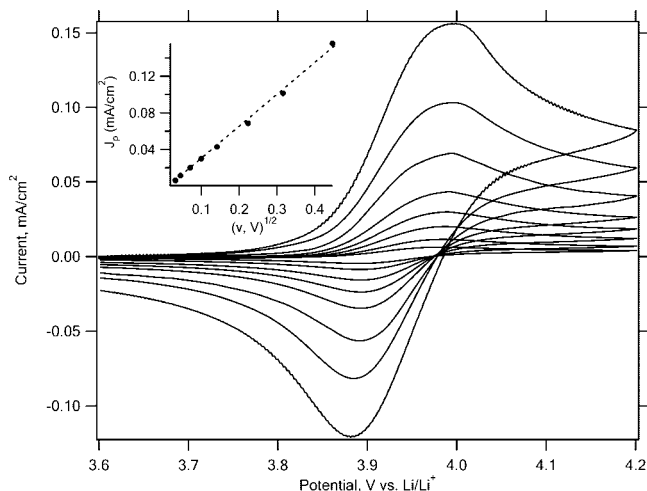
Figure 2 shows ten subsequent cyclic voltammograms of DW on TiO<sub>2</sub> at the slow scan rate (1 mV/s). The peak-to-peak splitting for the first scan was between 41 to 59 mV. The splitting is narrower than 60/ $n$  mV expected for a reversible redox system in solution, which indicates the surface confinement of DW. During repeated scanning, the integral voltammetric charge drops by ca. 2% per cycle and also the peak-to-peak splitting increases. This illustrates that there are certain limits of the stability of the DW/TiO<sub>2</sub> system at these conditions.

Figure 3 shows the cyclic voltammograms of DW adsorbed on the LiMnPO<sub>4</sub> electrode. The behavior is similar

(15) Wang, Q.; Zakeeruddin, S. M.; Nazeeruddin, M. K.; Humphry-Baker, R.; Grätzel, M. *J. Am. Chem. Soc.* **2006**, *128*, 4446.

(16) Wenseleers, W.; Stellacci, F.; Friedrichsen, T. M.; Mangel, T.; Bauer, C. A.; Pond, S. J. K.; Marder, S. R.; Perry, J. W. *J. Phys. Chem. B* **2002**, *106*, 6853.

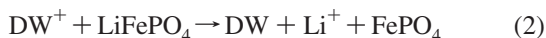
(17) Dahn, J. R.; Jiang, J.; Moshurck, L.; Fleischauer, M. D.; Buhrmester, C.; Krause, L. J. *J. Electrochem. Soc.* **2005**, *152*, A1283–A1289.



**Figure 3.** Cyclic voltammograms of DW adsorbed on a LiMnPO<sub>4</sub> electrode. Scan rates (in mV/s): 200, 100, 50, 20, 10, 5, 2, 1. Inset shows the forward peak current as a function of the square root of the scan rate.

to that on TiO<sub>2</sub> (cf. Figure 1). In other words, LiMnPO<sub>4</sub> mimics the behavior of an inert (insulating) support, and molecular wiring toward oxidative delithiation of LiMnPO<sub>4</sub> is absent. This is understandable because the available redox potential of DW does not provide enough driving force for this reaction. By using the same evaluation routine as for TiO<sub>2</sub> we can calculate the diffusion coefficient from the slope of  $J_p$  versus  $v^{1/2}$  (inset in Figure 3) to be  $D_+ = 3 \times 10^{-9}$  cm<sup>2</sup>/s. Interestingly, the cross-surface charge transport is approximately three times faster on LiMnPO<sub>4</sub> compared to TiO<sub>2</sub>. This might be due to different surface morphology: Whereas TiO<sub>2</sub> is a mesoporous material with statistically sintered 20-nm particles, the LiMnPO<sub>4</sub> consists of platelets of approximately 200 nm in size, exposing the (010) faces<sup>14</sup> on which the DW molecules can be assembled in a more ordered way. This enhances the intermolecular electronic coupling and hence the hole hopping rate.

Although LiMnPO<sub>4</sub> is inert for charging by DW via molecular wiring (cf. Figure 3), this effect is well apparent for LiFePO<sub>4</sub> olivine. Figure 4A shows that a constant current flows at potentials above approximately 4.1 V. This plateau (“wiring current”) is indicative for subsequent chemical reaction of the oxidized molecule (DW<sup>+</sup>) with LiFePO<sub>4</sub> olivine causing its oxidative delithiation:<sup>8</sup>



Interestingly, at faster scanning (200 mV/s) we can trace also the parent peaks of the DW redox couple, showing that a fast molecular charge transfer reaction foreruns the interfacial hole injection into LiFePO<sub>4</sub>. This kind of behavior was not yet reported for molecular wiring or targeting of LiFePO<sub>4</sub> (olivine).<sup>8,9,18</sup> At slower scanning (20 mV/s), the molecular couple is not seen, and the voltammogram is dominated by the catalytic wiring current only. Each curve in Figure 4A was acquired on a fresh electrode with roughly identical film’s mass and surface area. Also shown in Figure 4A is the behavior of a blank LiFePO<sub>4</sub> film, which was not treated by DW. This electrode shows negligible electro-

chemical activity, as expected for a stoichiometric olivine which is also free from any conductive carbon additives.

The surface coverage of LiFePO<sub>4</sub> with DW was analyzed spectrophotometrically (see Experimental Section) and found to be 0.5 nmol/cm<sup>2</sup> (referenced to the BET surface area of the electrode material), which is approximately 3 molecules/nm<sup>2</sup>. This surface coverage is similar to that found for TiO<sub>2</sub> (vide ultra) and also comparable to that reported for the BMABP/LiFePO<sub>4</sub> system: 2.5 molecules/nm<sup>2</sup>.<sup>8</sup> Hence, the surface concentration of 2–3 molecules/nm<sup>2</sup> seems to be representative for a monolayer coverage of these relatively small organic molecules with one phosphonic anchor. (Note that alternative molecular-wire molecules, viz., Ru–bipyridine complexes, occupy ca. 2 nm<sup>2</sup> per molecule<sup>18</sup> due to their larger size and different mode of surface attachment<sup>19</sup>).

The wiring current for the virgin electrode is not very dependent on the scan rate; this conclusion should be confronted with that of ref 8 (Supporting Information Figure S3) where a dependence was traced. Presumably, the gradual delithiation of LiFePO<sub>4</sub> during repeated cycling from faster to slower scan rates might, actually, have contributed to this effect (cf. ref 18). The voltammogram of partly delithiated electrode also shows more clearly that the wiring current is independent of the scan rate. Figure 4B presents the voltammogram of an electrode, which was delithiated by repeated cycling, followed by one-hour charging at a constant potential of 4.2 V. The total passed charge was equivalent to approximately 15% of the theoretical charge capacity (170 mAh/g) of the used electrode. This electrode still exhibits the wiring effect, albeit the current for the 15%-delithiated electrode is approximately 40 times smaller than for the fresh electrode.

To get further insight into the fading of wiring activity, we have tested the behavior of a fresh DW/LiFePO<sub>4</sub> electrode during 10 subsequent CV scans at various scan rates. Figure 5 summarizes the data for six electrodes; each plot at the given scan rate starts from a virgin electrode, while care was taken that all six electrodes had comparable areas and film masses ( $\approx 3$  mg/cm<sup>2</sup>). The molecular couple is still seen at the scan rate of 100 mV/s (cf. Figures 4 and 5). At the scan rates of 50 and 20 mV/s, we can trace an almost ideal molecular wiring behavior, which is also apparent at slower scanning of partly charged electrodes. Nevertheless, slower scanning of a virgin electrode confirms that the wiring current drops significantly already at the time scale of cyclic voltammetry. To be honest, the decrease of wiring current is not clearly understood at this stage of research. The obvious interpretation is that the presence of partly delithiated component in the LiFePO<sub>4</sub>/FePO<sub>4</sub> material (cf. refs 6 and 7) obstructs further reaction propagation. However, this argument would be equally applicable also for the “wiring” through graphitic carbon in the usual olivine cathodes. To address this problem, the different surface chemistry of molecular wiring and graphite wiring of LiFePO<sub>4</sub> needs to be taken into account.

We should note that our voltammograms of “good” molecular wiring, which are dominated by a constant current

(18) Kavan, L.; Exnar, I.; Cech, J.; Grätzel, M. *Chem. Mater.* **2007**, *19*, 4716.

(19) Kilsa, K.; Mayo, E. I.; Brunschwig, B. S.; Gray, H. B.; Lewis, N. S.; Winkler, J. R. *J. Phys. Chem. B* **2004**, *108*, 15640.

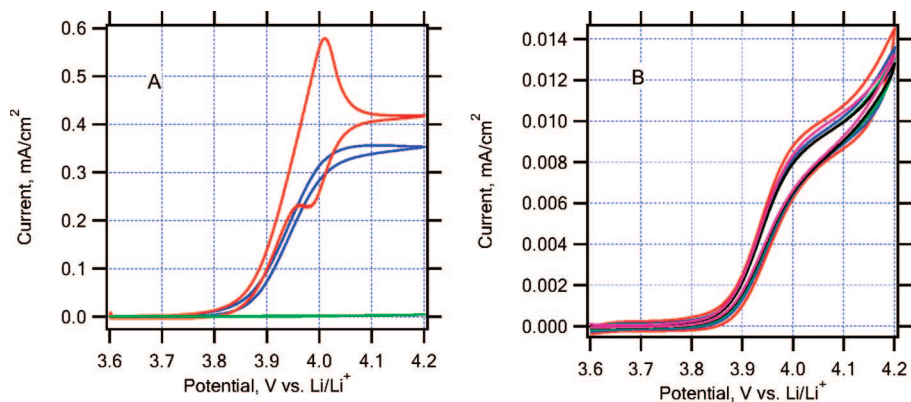


**Figure 4.** Cyclic voltammograms of DW-wired LiFePO<sub>4</sub> electrode. (A) Fresh electrode: first scan at 200 mV/s (red), 20 mV/s (blue). For comparison, green line is for LiFePO<sub>4</sub> electrode without DW (20 mV/s). (B) Used electrode (after 15% charge): scan rates (in mV/s): 20 (red), 10 (blue), 5 (green), 2 (black), 1 (magenta).

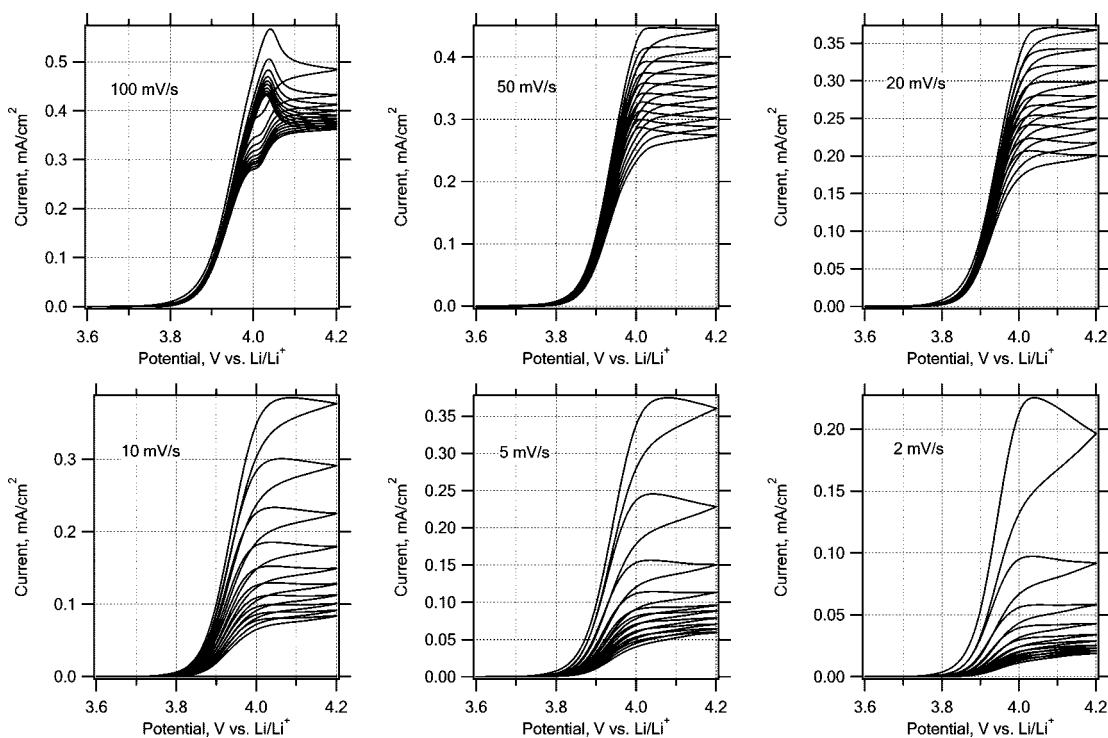


**Figure 5.** Cyclic voltammograms of a DW-wired LiFePO<sub>4</sub> electrode. Ten successive scans were accumulated for each given scan rate. The scanning started from a fresh electrode (ca. 3 mg/cm<sup>2</sup>).

at the anodic branch, are quite reminiscent of the behavior of DDB reported by Dahn et al.<sup>12</sup> Also in this case, an anodic plateau current is observed on slow voltammograms of DDB in solution. However, the physical reason for such a similarity is completely different. Whereas in the case of molecular wiring we deal with the effect of regenerating the reduced form of the couple after hole injection at the DW/LiFePO<sub>4</sub> interface, the anodic plateau seen by Dahn et al.<sup>12</sup> indicates that the condition of Randles–Sevcik semi-infinite diffusion is perturbed by regeneration of the redox couple at the counter electrode, that is, by the shuttle current flowing in the electrolyte solution. The latter is described by the Narayanan equation:<sup>12</sup>

$$I_{\text{shuttle}} = nFADc/L \quad (3)$$

where  $D$  and  $c$  are the diffusion coefficient and concentration of DDB in solution, respectively, and  $L$  is the distance between the working electrode and the counter-electrode. In

our case, the anodic plateau originated from the follow up chemical reaction (cf. 2) which is reminiscent of catalytic waves in classical electrochemistry.<sup>8</sup>

Figure 6 shows a potential-step chronoamperometry test of a virgin DW-wired LiFePO<sub>4</sub> electrode. The current is not linear with  $t^{-1/2}$ ; in other words, the Cottrell-like behavior is not traceable like for redox wiring of molecules on electrochemically inactive supports (TiO<sub>2</sub>).<sup>15</sup> This is quite understandable, because in our case, the chronoamperometry is not controlled by diffusion but by effects associated with the interfacial molecular wiring (cf. eq 2 and discussion above). Consequently, chronoamperometry allows evaluation of specific features of the wiring effect itself. During 1 h of constant charging at 4.2 V, we can pass a charge equivalent to approximately 12% of the total faradaic capacity of the electrode material (170 mAh/g). This is more explicitly shown by the inset of Figure 6, where the current is expressed in a way that is customary for battery testing. (Here, the C-rate stands for a convention

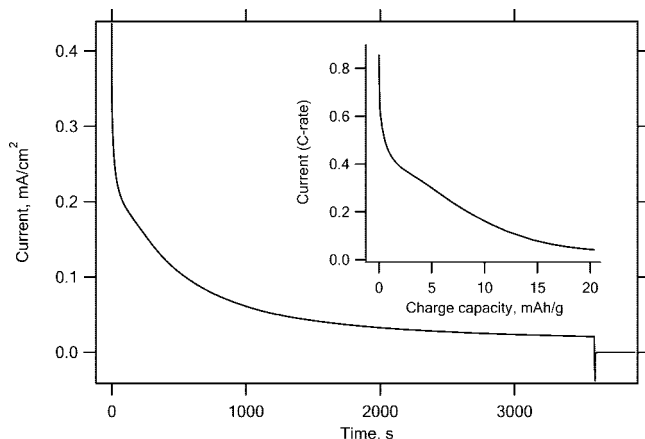


**Figure 6.** Potential-step chronoamperometry of a DW-wired LiFePO<sub>4</sub> electrode. The potential step was from 3.5 to 4.2 V (arrested for 3600 s) and subsequently back to 3.5 V (arrested for 300 s). Inset shows the same data recalculated in C-rate charging vs charge capacity of the actual electrode assuming 170 mAh/g as the theoretical charge capacity.

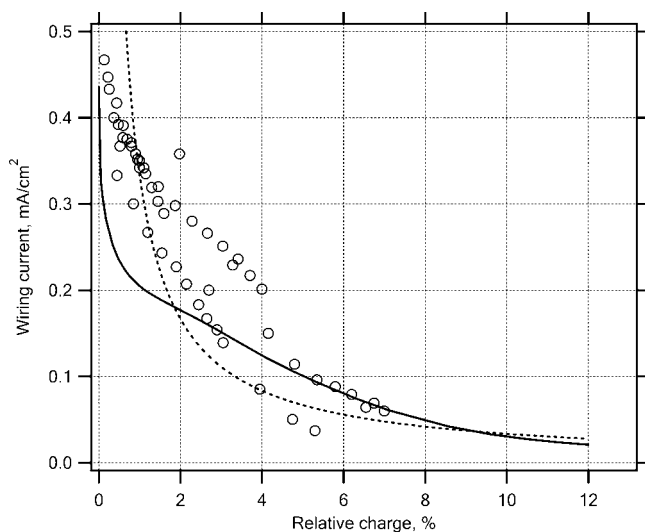


**Figure 7.** Compilation of the measured wiring currents as a function of the level of charging assuming 170 mAh/g (theoretical charge capacity) as the reference 100% charge. Points: data from CV at varying scan rates between 1 and 200 mV/s. Full line: data from potential-step chronoamperometry (3.5–4.2 V (3600 s)–3.5 V). Also shown is a model hyperbola (dashed line) assuming the wiring current was inversely proportional to the relative charge.

that 1C is a current for the full galvanostatic charging of the theoretical faradaic capacity during 1 h, that is, 170 mA/g for LiFePO<sub>4</sub>). Obviously, charging rates between C/2 and C/10 are realizable by molecular wiring of fresh electrodes and for shallow charging.

Our data confirm that the wiring current is primarily controlled by the state of the DW/LiFePO<sub>4</sub> interface, which is most easily described as the level of the LiFePO<sub>4</sub> charging. This is further presented on Figure 7, which compiles the data from cyclic voltammetry (plots like those in Figures 4 and 5) and chronoamperometry (Figure 6). Voltammetric data (points) and chronoamperometry data (full line) are reasonably matching. The wiring current is roughly inversely proportional to the level of discharge, and this is sketched by a dashed line in Figure 7.

The performance of a DW-wired LiFePO<sub>4</sub> olivine is far from that of the up-to-date carbon-coated LiFePO<sub>4</sub> cathodes

for Li-ion batteries. But it is certainly striking that a monolayer of molecules can carry sufficient currents for charging/discharging of conventional batteries. We can reasonably expect further performance enhancement by decreasing the particle size of the electrode material.

## Conclusions

A new redox-active molecule, [12-(2,5-di-*tert*-butyl-4-methoxy-phenoxy)-dodecyl]-phosphonic acid (coded DW), was synthesized. This molecule was designed on the basis of the earlier screening of redox-shuttles for overcharge protection in Li-ion batteries. The DW molecule is strongly anchored to the surfaces of TiO<sub>2</sub>, LiMnPO<sub>4</sub>, and LiFePO<sub>4</sub>. The coverage roughly corresponds to a monolayer with 2–3 molecules/nm<sup>2</sup>. DW exhibits good electrochemical stability at repeated redox cycling.

DW is reversibly oxidized at 3.95–4 V vs Li/Li<sup>+</sup>. If the substrate is redox inactive at these (or smaller) potentials (TiO<sub>2</sub>, LiMnPO<sub>4</sub>), we observe a reversible surface-confined electrochemistry of the chemisorbed DW/DW<sup>+</sup> couple. The cross-surface hole percolation is characterized by diffusion coefficients of  $(0.9 \text{ to } 3) \times 10^{-9} \text{ cm}^2/\text{s}$ , the higher value being for LiMnPO<sub>4</sub>.

The surface-anchored DW<sup>+</sup> interacts with LiFePO<sub>4</sub> (olivine) causing its oxidative delithiation. About 15% of the theoretical faradaic charge capacity can be extracted from the electrode material during several hours. The “molecular wiring” of virtually insulating electrode materials, like LiFePO<sub>4</sub>, consists in a charge transport from the current collector (FTO) to the olivine surface via the DW/DW<sup>+</sup> couple. The monomolecular layer of DW is capable of conducting holes across the LiFePO<sub>4</sub> (olivine) surface at the charging rates, which are of interest for practical Li-ion batteries (C/2–C/10 in early stages of discharging). The molecular wiring current is roughly inversely proportional to the level of olivine oxidation.

Although the performance of DW/LiFePO<sub>4</sub> is far from that of the carbon-coated LiFePO<sub>4</sub>, this paper shows that molecular addressing of olivine-based cathode materials is of principal interest for Li-ion batteries. There is a clear motivation for decreasing the amount of conductive carbonaceous additives in olivines, because carbon is just ballast in terms of charge (energy) density of the battery. Obviously, the molecular wiring represents the natural physical limit in minimizing the amount of conductive additives. Further performance enhancement is expected, if nanocrystalline olivines are used instead of the submicrometer sized crystals which were employed here. Further work is directed toward identifying novel molecular systems, which are capable of both cathodic and anodic molecular wiring of olivines.

**Acknowledgment.** This work was supported by HPL, SA, by the Czech Ministry of Education, Youth and Sports (Contract No. LC-510 and COST D35 1P05OC069), by Academy of Sciences of the Czech Republic (Contract No. IAA400400804), and by the Swiss National Science Foundation. We are grateful to Dr. Claudia Barolo for the synthesis of DW.